

# All-atom and coarse-grained simulations of the forced unfolding pathways of the SNARE complex

Wenjun Zheng\*

Department of Physics, University at Buffalo, State University of New York, New York

## ABSTRACT

The SNARE complex, consisting of three proteins (VAMP2, syntaxin, and SNAP-25), is thought to drive membrane fusion by assembling into a four-helix bundle through a zippering process. In support of the above zippering model, a recent single-molecule optical tweezers experiment by Gao *et al.* revealed a sequential unzipping of SNARE along VAMP2 in the order of the linker domain → the C-terminal domain → the N-terminal domain. To offer detailed structural insights to this unzipping process, we have performed all-atom and coarse-grained steered molecular dynamics (sMD) simulations of the forced unfolding pathways of SNARE using different models and force fields. Our findings are summarized as follows: First, the sMD simulations based on either an all-atom force field (with an implicit solvent model) or a coarse-grained Go model were unable to capture the forced unfolding pathway of SNARE as observed by Gao *et al.*, which may be attributed to insufficient simulation time and inaccurate force fields. Second, the sMD simulations based on a reparameterized coarse-grained model (i.e., modified elastic network model) were able to predict a sequential unzipping of SNARE in good agreement with the findings by Gao *et al.* The key to this success is to reparameterize the intrahelix and interhelix nonbonded force constants against the pair-wise residue–residue distance fluctuations collected from all-atom MD simulations of SNARE. Therefore, our finding supports the importance of accurately describing the inherent dynamics/flexibility of SNARE (in the absence of force), in order to correctly simulate its unfolding behaviors under force. This study has established a useful computational framework for future studies of the zippering function of SNARE and its perturbations by point mutations with amino-acid level of details, and more generally the forced unfolding pathways of other helix bundle proteins.

Proteins 2014; 00:000–000.  
© 2014 Wiley Periodicals, Inc.

**Key words:** coarse-grained model; dynamics; elastic network model; Go model; helix bundle; membrane fusion; SNARE; steered molecular dynamics; unfolding pathway; unzipping; zippering.

## INTRODUCTION

The soluble *N*-ethylmaleimide-sensitive factor attachment protein receptor (SNARE) proteins mediate membrane fusion in cells, particularly the fusion of vesicles in neurons to release neurotransmitters for synaptic transmission.<sup>1</sup> The neuronal SNARE consists of three proteins—vesicle-associated membrane protein 2 (VAMP2, also known as synaptobrevin) on the vesicle membrane (v-SNARE), and the binary complex of syntaxin 1 and Synaptosomal-associated protein 25 (SNAP-25) on the target plasma membrane (t-SNARE). The SNARE complex is thought to drive membrane fusion by assembling into a four-helix bundle (with one helix contributed by the t-SNARE syntaxin 1, a second by the v-SNARE VAMP2, and two more by the t-SNARE SNAP-25, see Fig. 1 and Ref. 2) through a zippering process<sup>2</sup>

from the N-termini toward the C-termini,<sup>3</sup> which generates a driving force that overcomes an energy barrier of over  $40 k_B T$  ( $k_B$ : Boltzmann's constant,  $T$ : temperature).<sup>4</sup> To probe the molecular basis of SNARE's membrane fusion function with amino-acid level of details,<sup>5</sup> it is critical to investigate the folding/unfolding process of SNARE under force with high spatial and temporal resolutions.

Additional Supporting Information may be found in the online version of this article.

Grant sponsor: NSF; Grant number: 0952736.

\*Correspondence to: Wenjun Zheng, Department of Physics, University at Buffalo, State University of New York, Buffalo, NY 14260.

E-mail: wjzheng@buffalo.edu

Received 16 October 2013; Revised 11 December 2013; Accepted 6 January 2014  
Published online 8 January 2014 in Wiley Online Library (wileyonlinelibrary.com). DOI: 10.1002/prot.24505

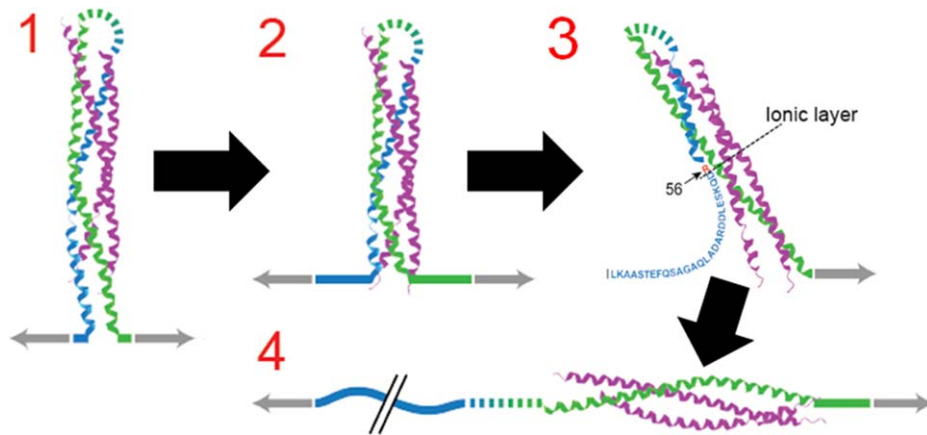


**Figure 1**

Four-state forced unfolding pathway of SNARE observed in a single-molecule optical tweezers experiment by Gao *et al.*<sup>6</sup> (reproduced with the permission of AAAS). Color scheme: VAMP2 (blue), syntaxin (green), SNAP-25 (purple). The gray arrows point to pulling directions, and the block arrows represent three transitions between four intermediate states (labeled by numbers 1–4).

In a recent single-molecule optical tweezers study,<sup>6</sup> Gao *et al.* observed the forced unzipping process of SNARE, which can be described by the following four-state unzipping model (Fig. 1)—the linker domain (LD), the C-terminal domain (Vc), and the N-terminal domain (Vn) of VAMP2 sequentially unzips away from the rest of SNARE core structure via three transitions (Fig. 1) with extension changes of 3, 7, and 15 nm, respectively. This model is consistent with many past experimental findings:

1. The t-SNARE and the v-SNARE (VAMP2) are partitioned between two separate membranes,<sup>7</sup> which are being pulled together during membrane fusion, hinting for the involvement of VAMP2 movement relative to the rest of SNARE complex.
2. The binary complex containing syntaxin and SNAP-25 is more stable than the binary complexes containing VAMP2 and either syntaxin or SNAP-25,<sup>8</sup> suggesting that VAMP2 is more susceptible to unzipping than syntaxin or SNAP-25.
3. While syntaxin is readily helical prior to SNARE assembly, VAMP2 is unstructured<sup>9</sup> or partially helical and partially disordered,<sup>10</sup> suggesting that VAMP2 is less stable and more susceptible to unfolding than syntaxin.
4. An analysis of surface interactions in an X-ray structure of SNARE shows significantly fewer interactions from the v-SNARE (VAMP2) than those from the t-SNARES,<sup>2</sup> consistent with the finding of stability analysis.<sup>8</sup>
5. Most of the known neurotoxin-mediated cleavage sites are concentrated in VAMP2 instead of syntaxin,<sup>11</sup> indicating the former may be structurally more extended/unfolded and therefore more susceptible to cleavage.

Despite the above supporting evidence, the structural details remain largely missing for those intermediate states of forced unfolding of SNARE (Fig. 1), which can only be resolved by direct structural studies at high resolution.

Structure-based molecular simulations (based on all-atom or simplified force field) are widely utilized to complement experimental efforts to study the energetics and dynamics of many biomolecular systems and processes, particularly the membrane fusion process mediated by SNARE.<sup>12–19</sup> The molecular dynamics (MD) simulation is capable of probing the dynamics of biomolecules under physiological conditions (i.e., in the presence of solvent and ions) with full atomistic details.<sup>20</sup> Previously, the unfolding dynamics and transition-state ensemble of a four-helix bundle were simulated by high-temperature MD,<sup>21</sup> and the steered MD<sup>22</sup> was used to simulate the extension of a three-helix bundle domain of myosin VI.<sup>23</sup> However, the all-atom MD simulations are computationally expensive and limited to 10s/100s of nanoseconds (ns) in simulation time, which is much shorter than the experimentally measured time-scale of synaptic vesicle fusion ( $\sim 60 \mu\text{s}$ <sup>24</sup>) and SNARE zippering ( $> \text{microsecond}$ <sup>6</sup>). Therefore, it is exceedingly difficult for MD simulations to adequately sample the conformational space and access key transitional intermediates of SNARE within limited simulation time. Additionally, the accuracy of MD force field for long-time simulations of protein dynamics is still uncertain even if such simulations were practical.

To speed-up MD simulations while retaining atomistic details, many venues have been attempted such as using implicit solvent model<sup>25</sup> instead of explicit solvent, or applying a driving force in steered MD,<sup>22</sup> and targeted MD,<sup>26</sup> and so forth. It is essential but difficult to ensure such manipulations do not substantially alter the intrinsic

dynamics of proteins during folding/unfolding and conformational transitions (e.g., see a recent study on the elimination of a bias in targeted MD simulations<sup>27</sup>). An alternative strategy is to use a coarse-grained model to reduce system size (e.g., treating an amino-acid residue as a coarse bead) and thereby the size of conformational space, which enables more efficient and extensive conformational sampling. A variety of coarse-grained models<sup>28</sup> have been developed to simulate protein conformational dynamics with high efficiency. For example, the elastic network model (ENM)<sup>29–31</sup> represents a protein structure as a network of  $C_\alpha$  atoms with neighboring ones connected by springs with a uniform force constant.<sup>32</sup> The normal mode analysis based on the ENM often yields good predictions of the collective motions favored by the native protein structure. To enable large conformational changes from an initial protein structure, we have recently adopted a modified form of the ENM (mENM) that uses harmonic interactions to maintain pseudo-bonds and secondary structure elements such as  $\alpha$ -helices, and an-harmonic interactions between nonbonded residues to allow them to move apart readily.<sup>33</sup> The mENM has proven useful in the flexible fitting of a high-resolution protein structure into low-resolution structural data such as cryo-electron-microscopy data<sup>33</sup> and solution X-ray scattering data.<sup>34</sup> Despite some success,<sup>35–40</sup> it remains uncertain if the coarse-grained models (including ENM and the Go model<sup>41</sup>) are sufficiently accurate to predict the correct sequence of conformational changes during protein folding/unfolding and conformational transitions.

To offer detailed structural insights to the unzipping process in SNARE, we have performed all-atom and coarse-grained steered molecular dynamics (sMD) simulations and analysis of the forced unfolding pathways of SNARE using different models and force fields. The goal of this study is two-fold: first, use molecular simulations (after proper reparameterization) to verify and substantiate the four-state unzipping model of SNARE proposed by Gao *et al.*<sup>6</sup>; second, use the observed forced unfolding pathway of SNARE<sup>6</sup> to critically assess the accuracy of various all-atom and coarse-grained models and force fields for simulating the forced unfolding pathways of helix bundle proteins represented by SNARE. This study has established a new mENM-based protocol for simulating the forced unfolding pathways of SNARE and other helix bundle proteins. In future studies, we will investigate how the unzipping/zippering activity of SNARE is affected by point mutations that perturb the membrane fusion function of SNARE.<sup>3</sup>

## METHODS

### All-atom sMD simulation of forced unfolding of SNARE

Following Brockwell *et al.*,<sup>42</sup> the all-atom sMD simulations were carried out using the CHARMM19 force field

and an implicit solvent model (EEF1),<sup>43</sup> which is computationally less expensive than using more state-of-the-art force field like CHARMM22 and explicit solvent. Therefore, we were able to perform more extensive sMD simulations given limited computing resource. An X-ray structure of SNARE complex (PDB id: 1SFC) was chosen as the initial conformation for sMD simulations. The protein was initially minimized in energy for 1000 steps using the ABNR algorithm, and then equilibrated for 20 ps prior to the productive sMD run. The pulling force was applied, via a spring of force constant 1000 pN/nm, to the  $C_\alpha$  atoms of residue L93 of VAMP2 and residue S259 of syntaxin to gradually increase their distance to 25 nm in 20 ns (pulling speed  $\sim 1.3$  nm/ns), using the AFM command<sup>44</sup> of the CHARMM program.<sup>45</sup> A harmonic distance restraint (with force constant  $100 \text{ kcal/mol/\AA}^2$ ) was added between the  $C_\alpha$  atoms of residue N25 of VAMP2 and residue S188 of syntaxin to mimic the disulfide bridge that crosslinked the N-termini of VAMP2 and syntaxin in Gao *et al.*<sup>6</sup> A Langevin dynamics simulation was run using the CHARMM program with a time step of 0.002 ps, a heat bath at 300 K temperature and a friction coefficient of  $0.1 \text{ ps}^{-1}$ . The atomic coordinates and pulling force were saved every 10,000 steps, resulting in 1000 snapshots saved for each 20 ns sMD trajectory. Thirty-two independent sMD trajectories were generated, and combined to form an ensemble of partially unfolded SNARE conformations for further analysis (see below).

### Go-model-based coarse-grained sMD simulation of forced unfolding of SNARE

The Go Model Server<sup>46</sup> of MMTSB ([mmtsb.org/web-services/gomodel.html](http://mmtsb.org/web-services/gomodel.html)) was used to generate the topology, parameter, and sequence files in CHARMM format for a  $C_\alpha$ -only Go model based on an X-ray structure of SNARE complex (PDB id: 1SFC). Then we adapted a sample CHARMM script for running a sMD simulation ([mmtsb.org/workshops/sean-bin\\_workshop\\_2012/Tutorial\\_s/Go\\_Pulling/GoModelPullingTutorial.html](http://mmtsb.org/workshops/sean-bin_workshop_2012/Tutorial_s/Go_Pulling/GoModelPullingTutorial.html)). The pulling force was applied, via a spring of force constant 1000 pN/nm, to the  $C_\alpha$  atoms of residue L93 of VAMP2 and residue S259 of syntaxin to gradually increase their distance to 25 nm in 100 ns (pulling speed  $\sim 0.25$  nm/ns), using the AFM command<sup>44</sup> of the CHARMM program.<sup>45</sup> A harmonic distance restraint (with force constant  $100 \text{ kcal/mol/\AA}^2$ ) was added between the  $C_\alpha$  atoms of residue N25 of VAMP2 and residue S188 of syntaxin to mimic the disulfide bridge that cross-linked the N-termini of VAMP2 and syntaxin in Gao *et al.*<sup>6</sup> A Langevin dynamics simulation was run using the CHARMM program with a time step of 0.01 ps, a heatbath at 300 K temperature and a friction coefficient of  $0.1 \text{ ps}^{-1}$ . The  $C_\alpha$  coordinates and pulling force were saved every 10,000 steps, resulting in 1000 snapshots for each 100 ns sMD trajectory. Thirty-two independent sMD trajectories were

generated, and combined to form an ensemble of partially unfolded SNARE conformations for further analysis (see below).

### Analysis of the ensemble of partially unfolded SNARE conformations

To analyze the forced unfolding pathway of SNARE, it is useful to calculate the reaction coordinate (RC) as the distance between the  $C_\alpha$  atoms of residue 93 of VAMP2 and residue 259 of syntaxin (named the pulling distance), which increases from 1 to 25 nm during the sMD simulations. All SNARE conformations were grouped by their RC values into a discrete set of RC bins (with bin width of 0.5 nm)—for example, the 4 nm RC bin consists of those SNARE conformations with  $3.75 \text{ nm} \leq \text{RC} \leq 4.25 \text{ nm}$ . An average conformation was calculated for each RC bin to represent that subset of SNARE conformations (after superimposing over the residues of SNAP-25). A movie consisting of a sequence of these average conformations in the order of ascending RC was generated to visualize the average unfolding pathway of SNARE under force. An average pulling force was calculated for each RC bin and plotted as a function of RC to obtain the force-distance relation as comparable to the pulling measurement in Gao *et al.*<sup>6</sup> To assess the extent of unfolding/unzipping at individual residue positions, we calculated the fraction of native interhelix contacts at residue  $i$  for a subset of  $N$  conformations from each RC

$$\text{bin: } f_i = \frac{\sum_n \sum_j \theta(1.1R_c - d_{ij,n})}{N \sum_j \theta(R_c - d_{ij,0})}, \text{ where } R_c \text{ is the cutoff}$$

distance of ENM,  $d_{ij,n}$  is the distance between residue  $i$  and  $j$  in conformation  $n$ ,  $d_{ij,0}$  is the distance between residue  $i$  and  $j$  in the native structure,  $\theta(x)$  is the Heaviside function, and the summation over  $j$  is limited to  $(i,j)$  residue pairs between different helices.

### Modified elastic network model (mENM)

A  $C_\alpha$ -only elastic network model (ENM) can be constructed from the atomic coordinates of a protein native structure. Each residue is represented by a bead located at its  $C_\alpha$  atom. The original form of the ENM potential energy<sup>32</sup> is

$$E_{\text{ENM}} = \frac{1}{2} \sum_{i < j} C_{ij} \theta(R_c - d_{ij,0}) (d_{ij} - d_{ij,0})^2, \quad (1)$$

where  $d_{ij}$  is the distance between residue  $i$  and  $j$ , and  $d_{ij,0}$  is the value of  $d_{ij}$  given by the native structure,  $\theta(x)$  is the Heaviside function,  $R_c$  is the cutoff distance,  $C_{ij}$  is the force constant of the spring connecting residue  $i$  and  $j$ .  $C_{ij}$  is usually set to a uniform constant for all residue pairs,<sup>30</sup> or two different values for bonded and nonbonded residue pairs.<sup>47</sup> By default, the force constant is

the same for all nonbonded pairs. But here for reparameterization we used two different force constants for nonbonded pairs within and between the helices of SNARE (see below).

To allow nonbonded residues to move apart readily while maintaining the pseudo-bonds between sequentially consecutive residues, we modified the ENM energy in Eq. (1) to the following form (named mENM energy)<sup>33,34</sup>:

$$E_{\text{mENM}} = E_b + E_{nb}$$

$$E_b = \frac{1}{2} \sum_{\langle ij \rangle \in P_b} C_b (d_{ij} - d_{ij,0})^2 \quad (2)$$

$$E_{nb} = \frac{1}{2} \sum_{\langle ij \rangle \notin P_b} C_{nb} \theta(R_c - d_{ij,0}) \times \frac{d_{ij,0}^2}{36} \left( 1 - \frac{d_{ij,0}^6}{d_{ij}^6} \right)^2$$

where  $E_b$  is the pseudo-bonded energy ( $P_b$  is the set of pseudo-bonded residue pairs, the bonded force constant  $C_b = 10 C_{nb}$ );  $E_{nb}$  is the nonbonded energy described by the Lennard-Jones 6–12 potential—it has a minimum at  $d_{ij,0}$ , saturates as  $d_{ij}$  goes to infinity, and diverges as  $d_{ij}$  approaches zero (here the nonbonded force constant  $C_{nb}$  can adopt two different values for residue pairs within and between the helices of SNARE, see below). Therefore, unlike the harmonic potential in Eq. (1), the mENM energy allows two nonbonded residues to move apart at a finite energy cost. In our previous studies based on the mENM,<sup>33,34</sup> we used harmonic interactions to maintain secondary structure elements like  $\alpha$ -helices and  $\beta$ -strands,<sup>33,34</sup> which were not used here to allow the unfolding of helices in SNARE.

The mENM energy in Eq. (2) can be expanded near a given conformation  $X_*$  to the second order as follows:

$$E_{\text{mENM}}(X) \approx E_{\text{mENM}}(X_*) + \delta X^T G + \frac{1}{2} \delta X^T H \delta X, \quad (3)$$

where  $\delta X = X - X_*$ ,  $G = \nabla E_{\text{mENM}}|_{X=X_*}$  is the gradient of  $E_{\text{mENM}}$  at  $X = X_*$ , and  $H$  is the  $3N \times 3N$  Hessian matrix comprised of the following  $3 \times 3$  blocks:

$$H_{ij} = \begin{bmatrix} \left. \frac{\partial^2 E_{\text{mENM}}}{\partial x_i \partial x_j} \right|_{X=X_*} & \left. \frac{\partial^2 E_{\text{mENM}}}{\partial x_i \partial y_j} \right|_{X=X_*} & \left. \frac{\partial^2 E_{\text{mENM}}}{\partial x_i \partial z_j} \right|_{X=X_*} \\ \left. \frac{\partial^2 E_{\text{mENM}}}{\partial y_i \partial x_j} \right|_{X=X_*} & \left. \frac{\partial^2 E_{\text{mENM}}}{\partial y_i \partial y_j} \right|_{X=X_*} & \left. \frac{\partial^2 E_{\text{mENM}}}{\partial y_i \partial z_j} \right|_{X=X_*} \\ \left. \frac{\partial^2 E_{\text{mENM}}}{\partial z_i \partial x_j} \right|_{X=X_*} & \left. \frac{\partial^2 E_{\text{mENM}}}{\partial z_i \partial y_j} \right|_{X=X_*} & \left. \frac{\partial^2 E_{\text{mENM}}}{\partial z_i \partial z_j} \right|_{X=X_*} \end{bmatrix},$$

where  $x_i, y_i, z_i$  ( $x_j, y_j, z_j$ ) is the  $x, y, z$ -coordinate of residue  $i$  ( $j$ ). The gradient and Hessian matrix is used in the minimal-energy pathway modeling protocol (see below).

### mENM-based minimal-energy pathway modeling of forced unfolding of SNARE

To explore minimal-energy conformations of partially unfolded SNARE under force, we minimize a pseudo-energy  $E_{total}$ , which is the sum of the following three components—the mENM energy  $E_{mENM}$  based on the native structure [Eq. (2)], a collision energy  $E_{col}$  (see below), a random-coil energy  $E_{coil}$  (see below), and a harmonic distance-restraint score  $E_{pull}$  for pulling two given residues toward a target distance (see below):

$$E_{total} = E_{mENM} + E_{pull} + E_{col} + E_{coil}, \quad (5)$$

$$E_{col} = \frac{1}{2} \sum_{i < j} C_{col} \theta(d_{ij,0} - R_c) \theta(R_{col} - d_{ij}) (d_{ij} - R_{col})^2, \quad (6)$$

where the collision force constant  $C_{col} = 10 C_{nb}$ ,  $R_{col}$  is the minimal distance between two nonbonded residues in the native structure.<sup>33,47</sup> The addition of  $E_{col}$  penalizes steric collisions between nonbonded residues, which are within a distance of  $R_{col}$  and do not form nonbonded contact in the native structure.

$$E_{coil} = \frac{1}{2} \sum_i C_{coil} \theta(d_{i,i+2} - R_{coil}) (d_{i,i+2} - R_{coil})^2, \quad (7)$$

where a harmonic pulling force between residue  $i$  and  $i + 2$  (with force constant  $C_{coil} = 10 C_{nb}$ ) is turned on if their distance  $d_{i,i+2} > R_{coil} = 6 \text{ \AA}$ . This is to ensure that an unfolded random coil is not locally over-stretched.

$$E_{pull} = 0.5 C_{pull} [d_{pull} - d_{target}(\lambda)]^2, \quad (8)$$

where the pulling force constant is  $C_{pull} = 10 C_{nb}$ , the target distance  $d_{target}(\lambda) = \lambda d_{init} + (1 - \lambda) d_{end}$  is a linear interpolation between the initial value ( $\sim 1 \text{ nm}$ ) and final value ( $\sim 25 \text{ nm}$ ) of the pulling distance  $d_{pull}$ , and  $\lambda \in [0, 1]$  is the interpolation parameter. The pulling force is calculated as follows:

$$F = C_{pull} |d_{pull} - d_{target}(\lambda)|. \quad (9)$$

To simulate the unfolding pathway of SNARE upon a slow constant-speed pulling at zero temperature, we gradually decreased  $\lambda$  from 1 to 0, and for each given  $\lambda$ , we minimize the pseudo-energy in Eq. (5). We employed the Newton-Raphson algorithm to solve  $\nabla E_{total}(\lambda, X_{min}) = 0$  by using the following iterative procedure:

1. Initialization: set  $n = 0$ ,  $\lambda_0 = 1$ , and  $X_0 = X_{min,0} = X_{nat}$ , where  $X_{nat}$  represents the  $C_\alpha$  coordinates of the native structure.
2. If  $n > 0$ , set  $\lambda_n = \lambda_{n-1} - 0.01$ .
3. For conformation  $X_n$ , calculate the pseudo-energy  $E_n$  using Eq. (5), then set  $X_{min,n} = X_n$  if  $E_n$  reaches a new low.

4. For conformation  $X_n$ , calculate the gradient  $\nabla E_{total}$ ; if  $|\nabla E_{total}| < 0.00001$  stop minimization and go to Step 7.
5. Displace  $X_n$  by the following incremental displacement:

$$\delta X_n = -(H_{mENM} + H_{pull} + H_{col} + H_{coil})^{-1} \nabla E_{total}, \quad (10)$$

where  $H_{mENM}$ ,  $H_{pull}$ ,  $H_{coil}$  and  $H_{col}$  are the Hessian matrices calculated from  $E_{mENM}$ ,  $E_{pull}$ ,  $E_{coil}$  and  $E_{col}$ , respectively [Eq. (5)].

6. Go to Step 3.
7. Stop if  $\lambda_n = 0$ .
8. Set  $n \leftarrow n + 1$  and  $X_n = X_{min,n} = X_{min,n-1}$ , then go to Step 2.

To reduce accumulation of structural distortions, we limit the magnitude of each incremental displacement [Eq. (10)]  $\leq 0.2 \text{ \AA}$  in the root mean squared deviation. This is attained by adding  $\varepsilon I$  (where  $I$  is an identity matrix and  $\varepsilon$  is an adjustable parameter) to the sum of Hessian matrices such that the linear-equation solution in Eq. (10) satisfies this condition.

### Reparameterization of mENM based on pair-wise distance fluctuations

To enable reparameterization with minimal addition of new parameters, we allowed the nonbonded force constant to have two different values:  $C_{ij} = C_{nb}$  if residue  $i$  and  $j$  are in the same helix, and  $C_{ij} = w C_{nb}$  if residue  $i$  and  $j$  are in different helices. To determine the parameters  $R_c$ ,  $C_{nb}$ , and  $w$  of mENM for SNARE, we used the following procedure:

1. We ran ten 10 ns MD simulations of SNARE using the CHARMM19 force field and the EEF1 implicit solvent model (same MD setup as the sMD simulations but in the absence of pulling force, see above), then kept 1000 snapshots from each MD trajectory to form a 10,000-snapshot ensemble of folded conformations of SNARE.
2. We calculated the following root mean squared fluctuation (RMSF) for all residue-residue pair-wise distances based on the above ensemble:

$$\sigma_{ij}^{MD} = \sqrt{\frac{1}{N} \sum_{n=1}^N |d_{ij,n} - \langle d_{ij} \rangle|^2}, \quad (11)$$

where  $d_{ij,n}$  is the distance between the  $C_\alpha$  atoms of residue  $i$  and  $j$  in snapshot  $n$ ,  $\langle d_{ij} \rangle = \frac{1}{N} \sum_{n=1}^N d_{ij,n}$ ,  $N = 10,000$  is the total number of snapshots.

3. We calculated the following RMSF for all residue-residue pair-wise distances based on the normal mode analysis of the mENM energy:

$$\sigma_{ij}^{\text{mENM}} = \sum_m \frac{|\delta d_{ij,m}|^2}{\lambda_m}, \quad (12)$$

where  $\delta d_{ij,m}$  is the change in  $d_{ij}$  given by the eigenvector of mode  $m$ , and  $\lambda_m$  is the eigenvalue of mode  $m$ .

4. We searched all combinations of  $R_c \in [8 \text{ \AA}, 15 \text{ \AA}]$  and  $w \in (0, 1]$  to minimize  $\sum_{i < j} |\sigma_{ij}^{\text{MD}} - \sigma_{ij}^{\text{mENM}}|^2$  using linear regression.

### mENM-based sMD simulation of forced unfolding of SNARE

To explore the forced unfolding pathways of SNARE upon constant-speed pulling at room temperature using the mENM force field, we performed sMD simulations with the CHARMM program. To incorporate the mENM parameters, we modified the Go-model parameter file (obtained from the Go Model Server, see above) by replacing the native nonbonded Lennard-Jones parameters of Go model with the mENM non-bonded parameters [Eq. (2)]. Then we ran 32 sMD simulations similar to those based on the Go model (see above), and then performed the same analysis of average pathway and force-distance relation (see above).

## RESULTS AND DISCUSSION

### All-atom sMD simulation of forced unfolding pathways of SNARE

To explore the forced unfolding pathways of the SNARE complex in comparison with Gao *et al.*,<sup>6</sup> we used the sMD simulation method<sup>22</sup> to simulate constant-speed pulling of two C-terminal residues of SNARE via a harmonic spring (see Methods section). Our sMD simulations started from a four-helix bundle structure of SNARE solved by X-ray crystallography (PDB id: 1SFC). Following the optical tweezers experiment in Gao *et al.*,<sup>6</sup> the C-terminal residue L93 of VAMP2 and the C-terminal residue S259 of syntaxin were being pulled apart with their distance (named pulling distance) increasing toward 25 nm (sum of 3, 7, and 15 nm extension changes as observed in Gao *et al.*<sup>6</sup>) in 20 ns time. The disulfide bridge between the N termini of syntaxin and VAMP2<sup>6</sup> was modeled by a harmonic distance restraint (see Methods section).

To extensively sample the diversity of forced unfolding pathways of SNARE, we generated 32 independent sMD runs. In 27 runs, syntaxin was unzipped all the way up to its N-terminal  $\sim 10$  residues while VAMP2 was only partially unfolded in the LD (residues 85–93); only in 4 runs was VAMP2 unzipped all the way up to the Vn domain while syntaxin was only partially unfolded. Therefore, the all-atom sMD simulations predicted that

the forced unfolding of SNARE is dominated by syntaxin unfolding rather than VAMP2 unfolding, which was evident in the average unfolding pathway (i.e., a sequence of average conformations of partially unfolded SNARE sorted in the order of ascending pulling distance, see Methods and movie S1, Supporting Information). In the average unfolding pathway, the minority contributions of VAMP2-unfolding pathways led to an upward movement and shortening of the Vc domain of VAMP2 (see movie S1, Supporting Information). To further visualize the variations among partially unfolded conformations of SNARE, we have shown a conformational ensemble of SNARE with the pulling distance falling within 0.25 nm of 11 nm [Fig. 2(a)], and their average conformation [Fig. 2(b)], corresponding to the “half-zipped” state 3 in Gao *et al.*<sup>6</sup> (Fig. 1). This ensemble is clearly dominated by conformations featuring slight unfolding of VAMP2 and substantial unfolding of syntaxin [with residue S259 pulled much closer to the N-termini than L93 in Fig. 2(a)], whereas only a minority of conformations feature slight unfolding of syntaxin and substantial unfolding of VAMP2 [with residue L93 pulled much closer to the N-termini than S259 in Fig. 2(a)].

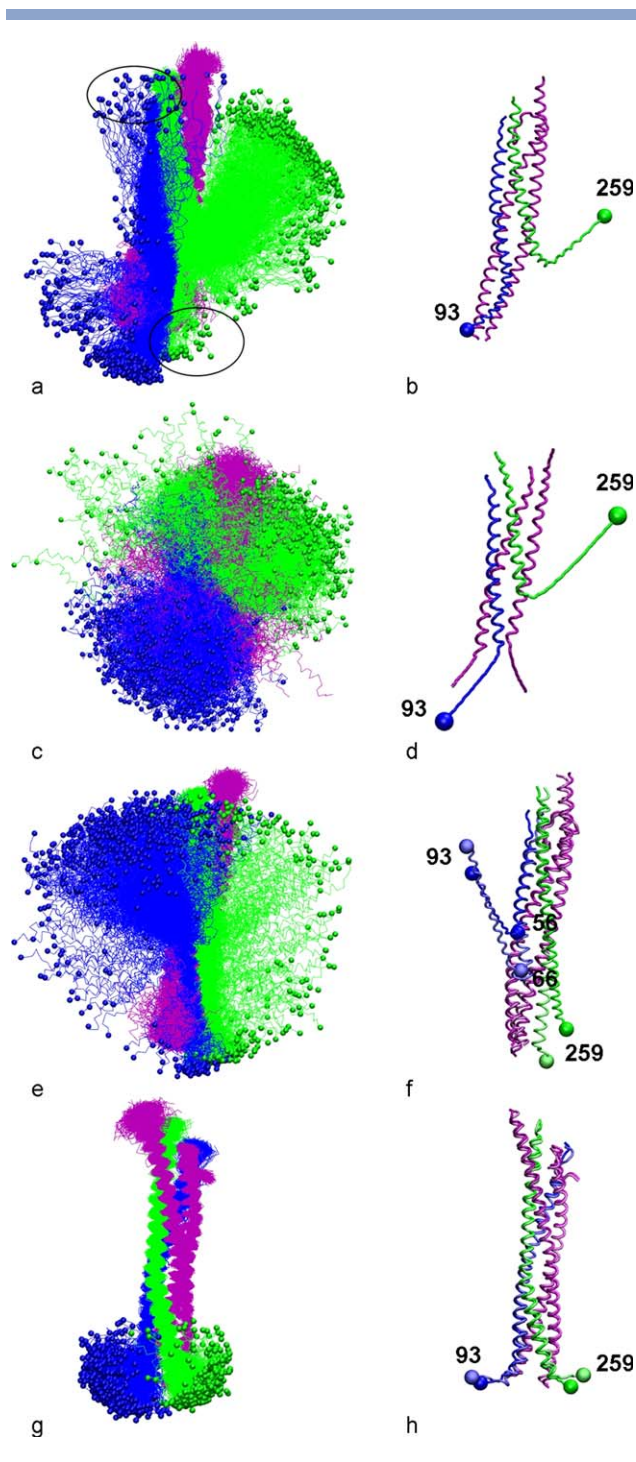
The above finding contradicted the experimental finding by Gao *et al.*<sup>6</sup> that VAMP2 is sequentially unzipped toward its Vn domain while syntaxin is only partially unfolded, raising doubt about the validity of all-atom sMD simulation (with implicit solvent) in predicting forced unfolding pathways of SNARE. Although sMD was previously used to simulate forced unfolding of various proteins,<sup>42,44,48,49</sup> to our knowledge, it was never systematically validated for helix bundle proteins in comparison with the partially unfolded intermediates revealed by single-molecule pulling measurements.

One likely reason for the failure of sMD to agree with single-molecule pulling experiment<sup>6</sup> is because of the mismatch in pulling time-scale and speed—our sMD simulation of pulling was completed in 20 ns (speed = 1.3 nm/ns) while the pulling experiment in Gao *et al.*<sup>6</sup> took  $\sim$ seconds (speed = 10 nm/s). Therefore, the sMD simulation may be too fast to sample the equilibrium intermediate states accessible to the experimental pulling measurements of SNARE in Gao *et al.*<sup>6</sup> To address this issue under the constraint of our computing resource, we ran 32 longer sMD simulations with the pulling distance increasing toward 11 nm in 40 ns, so the pulling speed was reduced by  $\sim 5$ -fold. The resulting average unfolding pathway was still dominated by syntaxin unfolding similar to the finding by faster 20 ns sMD (see movie S2, Supporting Information). Therefore, the pulling speed may not be the only main factor that affects the forced unfolding pathways of SNARE. Another possible factor is the inaccuracy of all-atom force field for sMD simulation. Although the all-atom force-field parameters (including CHARMM19 as used here) were well calibrated and tested for energetics and fast

dynamics of peptides and small proteins (fs-ns in time scale), their accuracy for long-time dynamics (ns-s in time scale) remains uncertain. For instance, certain non-bonded interactions (such as those at crystal contacts in protein crystals) need to be rescaled to optimally describe the atomic fluctuations as measured in X-ray crystallography.<sup>50</sup> Unfortunately, owing to their sophistication,

all-atom force fields often lack the flexibility for convenient reparameterization.

One way to address the above two issues with all-atom sMD is to perform coarse-grained sMD simulation, which is computationally inexpensive and based on simple force field, so it may allow for longer simulation time and flexible reparameterization.



### Coarse-grained sMD simulation of forced unfolding pathways of SNARE based on the Go model

The Go model, a  $C_{\alpha}$ -only model constructed based on the residue–residue contacts in a protein native structure, has been extensively used to simulate protein folding and unfolding.<sup>41</sup> To simulate the forced unfolding pathways of SNARE, we performed coarse-grained sMD simulation based on the Go-model force field (see Methods section). Our sMD simulations started from the same four-helix bundle structure of SNARE as used for all-atom sMD (see above). Following Gao *et al.*,<sup>6</sup> residue L93 of VAMP2 and S259 of syntaxin were being pulled apart with their distance (named pulling distance) increasing toward 25 nm in 100 ns time. The use of Go model allowed us to simulate pulling at 5-fold lower speed than the all-atom sMD.

In all 32 sMD runs, both the C-termini and N-termini of the four helices seemed to be highly flexible and partially unfolding [Fig. 2(c)], and the entire four helix bundle (including SNAP-25) started to disassemble at pulling distance  $\sim 11$  nm. The pulling force seemed to affect syntaxin the most, which was unzipped toward its N-terminus, while VAMP2 and SNAP-25 were partially unfolding without unzipping toward their N-termini [Fig. 2(d) and movie S3, Supporting Information]. This finding was qualitatively similar to that of all-atom sMD despite differences in pulling speed and force field, and both contradicted the experimental finding that VAMP2 is sequentially unzipped toward its Vn domain while syntaxin is only partially unfolded in Gao *et al.*<sup>6</sup> These negative results indicate that sMD simulation based on commonly used all-atom or coarse-grained force fields

### Figure 2

An ensemble of partially unfolded conformations of SNARE with pulling distance  $\sim 11$  nm obtained by all-atom sMD simulation (a), Go-model-based sMD simulation (c), mENM-based sMD simulation (e), and the ensemble with pulling distance  $\sim 4$  nm by mENM-based sMD simulation (g). The corresponding average conformations are shown in panels (b), (d), (f), and (h). The following color scheme is used: VAMP2 (blue), syntaxin (green), SNAP-25 (purple). The SNARE complex is in an upright position with its N/C-termini at the top/bottom. In the ensemble view, residue L93 and S259 are represented by blue and green spheres, respectively. In panel (a), the positions of residue L93 and S259 in those conformations linked to the VAMP2-unfolding pathway are circled. In panel (f) and (h), the corresponding minimal-energy conformations are also shown with lighter colors.

may not be accurate enough to capture the forced unfolding pathways of SNARE and other proteins.

### Coarse-grained modeling of forced unfolding pathways of SNARE based on the reparameterized mENM

To correctly model the forced unfolding pathways of SNARE, we have adopted the strategy of reparameterizing an existing coarse-grained model using dynamics data from all-atom MD simulations. The coarse-grained model used here is a modified version of the ENM (mENM) where the harmonic interactions between nonbonded residue pairs are replaced by an-harmonic forces in the form of a Lennard–Jones potential.<sup>34,51</sup> (see Methods section). Compared with the original ENM, the mENM allows nonbonded residue–residue contacts to break apart more readily to facilitate large conformational changes.<sup>34,51</sup> For reparameterization, we have assigned two different nonbonded force constants— $C_{nb}$  for nonbonded pairs within each helix, and  $wC_{nb}$  for those between helices, where  $w$  is a weight factor within [0,1] (see Methods section). We tuned  $w$ ,  $C_{nb}$ , and  $R_c$  to optimize the fitting of residue–residue distance fluctuations obtained from all-atom MD simulations (see Methods section). Interestingly, the optimization yielded  $w = 0.2$ ,  $C_{nb} = 0.16$  kcal/mol/Å<sup>2</sup> and  $R_c = 13$  Å, suggesting relatively weaker interhelix interactions than those intrahelix ones. So the helices of SNARE should be effectively “rigidified” to better capture their dynamic fluctuations in the absence of force. Similar ideas were proposed and tested in the literature of ENM, such as enhancing the rigidity of domains by using a larger spring constant for intradomain contacts,<sup>52</sup> and weakening the interprotein contacts to improve the modeling of anisotropic atomic fluctuations in protein crystals.<sup>53</sup> Like those earlier studies, the above reparameterization helps to enhance the cohesiveness of protein structures, which is not fully accounted for by existing all-atom force-fields without multibody interactions.<sup>54,55</sup>

To assess if the above new mENM parameters can be used to obtain the correct unfolding pathway of SNARE, we have developed and applied a mENM-based protocol for minimal-energy pathway modeling (see Methods section). Using this protocol, we generated a sequence of minimal-energy intermediate conformations of SNARE as the pulling distance gradually increases to 25 nm (see Methods and movie S4, Supporting Information), which mimics near-equilibrium forced unfolding of SNARE at zero temperature (i.e., without thermal fluctuations). Encouragingly, we have observed two distinct stages of structural transitions similar to Gao *et al.*<sup>6</sup>:

1. Simultaneous unfolding/unzipping of the LD of VAMP2 and the C-terminal ~5 residues of syntaxin at pulling distance ~4 nm [see Fig. 2(h)], which corresponds to the LD unfolding transition (state 1 → state

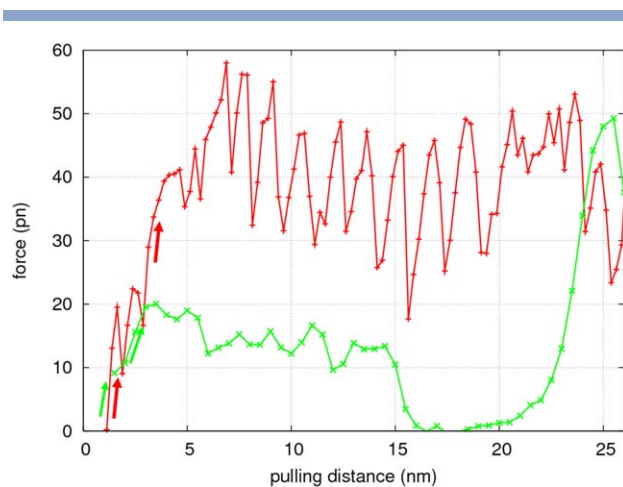


**Figure 3**

Pulling force as a function of pulling distance (i.e., the distance between residue L93 of VAMP2 and S259 of syntaxin) obtained from minimal-energy pathway modeling (+) and sMD simulations (x) based on the mENM. The transitions are indicated by arrows. [Color figure can be viewed in the online issue, which is available at [wileyonlinelibrary.com](http://wileyonlinelibrary.com).]

- 2, see Fig. 1) with 3 nm change of extension as observed in Gao *et al.*<sup>6</sup>
2. Further unfolding/unzipping of the Vc domain of VAMP2 up to residue R66 at pulling distance ~11 nm [Fig. 2(f)], which corresponds to the Vc unfolding transition (state 2 → state 3, see Fig. 1) with 7 nm change of extension as observed in Gao *et al.*<sup>6</sup> Notably, the Vc unfolding was ~10 residues short of reaching residue 56 at the central ionic layer of the SNARE complex [Fig. 1]. This is due to the lack of thermal fluctuations, which would have caused further unfolding/unzipping of the Vc domain (see below). Indeed, the unfolded Vc domain adopted a regular zig-zag conformation, which would have been more disordered in the presence of thermal fluctuations [Fig. 2(f)].

Next, we analyzed the relation between pulling force and pulling distance based on the minimal-energy pathway modeling (see Methods section). We observed two distinct transitions in the force-distance relation (Fig. 3)—one toward a low-force (10–20 pN) region near 1 nm, and another toward a high-force (20–50 pN) region near 3–4 nm: in the low-force region, the pulling distance varies within 1–3 nm; in the high-force region, the pulling distance varies within 4–26 nm. The above transitions correspond to similar transitions found by Gao *et al.*<sup>6</sup>—first transition to a LD-unfolded state (state 1 → state 2, Fig. 1) with 3 nm extension change and low force (8–13 pN), and second transition to a Vc-unfolded state (state 2 → state 3, Fig. 1) with 7 nm extension change and high force (14–19 pN). The higher calculated force than experimental force may be attributed to the

absence of thermal fluctuations, which would favor unfolding and lower unfolding force. The sharp peaks in the calculated force-distance curve (Fig. 3) are due to sequential unwinding of helical turns in VAMP2.

In sum, thanks to the reparameterization of mENM, we have captured the forced unfolding pathway of SNARE featuring sequential unzipping of LD, Vc, and Vn of VAMP2, in qualitative agreement with Gao *et al.*<sup>6</sup> Additionally, the pulling force switches from low force to high force during unfolding, which resembles the force-extension behavior observed in Gao *et al.*<sup>6</sup> For comparison, we have performed the same pathway modeling using the ENM with uniform nonbonded force constant (i.e.,  $w = 1$ ), which predicted more extensive unzipping of syntaxin than VAMP2 (see movie S5, Supporting Information), similar to the findings of all-atom and Go-model-based sMD simulations (see above).

### Coarse-grained sMD simulation of mechanical unfolding pathways of SNARE based on the reparameterized mENM

To further probe the forced unfolding pathways of SNARE in the presence of thermal fluctuations, we conducted sMD simulation based on the reparameterized mENM (see Methods section). The sMD simulations started from the same four-helix bundle structure of SNARE as used for all-atom and Go-model-based sMD (see above). Following Gao *et al.*,<sup>6</sup> residue L93 of VAMP2 and S259 of syntaxin were being pulled apart with their distance increasing toward 25 nm in 100 ns time. We generated 32 independent sMD runs (see movie S7, Supporting Information). In 29 runs, VAMP2 was unzipped all the way up to its Vn domain while syntaxin was only partially unfolded in the C-terminal region; only in 3 runs was syntaxin unzipped all the way up to its N-terminus while VAMP2 was only partially unfolded. The dominance of VAMP2-unfolding pathways was evident in the average unfolding pathway (see movie S6, Supporting Information), where the minority contribution of syntaxin-unfolding pathways led to an upward movement and shortening of syntaxin [Fig. 2(f) and movie S6, Supporting Information]. This finding qualitatively agrees with the experimental finding of sequential unzipping of VAMP2 instead of syntaxin in Gao *et al.*<sup>6</sup>

We then focused on two intermediate states of partially unfolded SNARE at pulling distance of 4 nm and 11 nm, corresponding to state 2 and 3 of Gao *et al.*<sup>6</sup> (Fig. 1).

1. At pulling distance  $\sim 4$  nm, both VAMP2 and syntaxin were unzipped almost equally [Fig. 2(g,h)], involving residues 82–93 of VAMP2's LD and residues 253–259 of syntaxin (with  $>80\%$  native interhelix contacts lost, Supporting Information Fig. S1a), which is in agreement with the finding of state 2 in Gao *et al.*<sup>6</sup>

2. At pulling distance  $\sim 11$  nm, VAMP2 was further unfolded/unzipped up to residue 59 [Fig. 2(e,f)] while syntaxin's unfolding was limited to residues 251–259 (with  $>80\%$  native interhelix contacts lost, Supporting Information Fig. S1b), which is in agreement with the finding of state 3 in Gao *et al.*<sup>6</sup> The core residues of these partially unfolded conformations consist of residues 34–48 of VAMP2, 204–218 of syntaxin, 23–51 and 140–166 of SNAP-25 (with  $>80\%$  native interhelix contacts retained, Supporting Information Fig. S1b).

Next, we analyzed the force-distance relation based on the mENM-based sMD simulations, where the pulling forces for those conformations within the same pulling distance bins were averaged to reduce noise (Fig. 3). Similar to the minimal-energy pathway, we found two transitions—one toward a low-force ( $\sim 10$  pN) region near  $\sim 1$  nm, and another toward a high-force (10–20 pN) region near  $\sim 3$  nm. The values of calculated force were comparable to the experimental force values.<sup>6</sup> In addition, there was a sudden drop of force at  $\sim 15$  nm coinciding with the melting of Vn domain and complete unfolding of VAMP2, and a rise of force in 20–26 nm due to the stretching of unfolded VAMP2 and its cross-linker with syntaxin.

In sum, our sMD simulations based on the reparameterized mENM successfully captured the dominant route of the forced unfolding pathways of SNARE—sequential unzipping of LD (with low force), Vc (with high force), and Vn of VAMP2, in good agreement with Gao *et al.*<sup>6</sup> Compared with the result of minimal-energy pathway modeling, both VAMP2 and syntaxin were more flexible and susceptible to forced unzipping [Fig. 2(e,g)], although the VAMP2 unzipping dominated the unfolding pathways of SNARE [Fig. 2(f)].

### Lesson for molecular simulations of forced unfolding pathways of proteins

Despite many years of simulation studies of mechanical unfolding of various proteins, the commonly used all-atom and coarse-grained force fields still lack the accuracy needed to correctly predict the forced unfolding pathways of even a small protein like a four-helix bundle. This study has demonstrated a promising venue to improve such simulations via the reparameterization of a coarse-grained model (such as mENM) based on all-atom dynamics data. This strategy allows flexible adaptation of simple coarse-grained force field to specific protein systems. Despite the added computing overhead for collecting dynamics data and running reparameterization, this strategy may be well justified considering the positive impact of more accurate simulations on functional study and the more challenging alternative of developing/refining a generic force field for all proteins.<sup>56</sup> Future studies will be needed to further establish the

general applicability of this strategy for other helical bundle proteins.

### Relevance to functional study of SNARE

Our simulations strongly support the functional importance of the inherent flexibility/dynamics of the SNARE complex, which must be accurately modeled via reparameterization in order to correctly capture its unzipping behavior. Indeed, higher flexibility of the SNARE helices was previously observed in the N/C-terminal regions by a structural study.<sup>2</sup> The propensity of VAMP2 to unzip/unfold under force, as revealed by both pulling experiment<sup>6</sup> and sMD simulation (this study), is desirable in order to fulfill the membrane fusion function of SNARE (i.e., forcibly joining vesicles and target membranes together).<sup>2</sup> As suggested by both Gao *et al.*<sup>6</sup> and our simulation, the high force generated during Vc unzipping and zipping supports the key role of this transition as the major powerstroke for membrane fusion.<sup>57</sup> Indeed, from the force-distance relation derived based on our sMD simulations, we found a pulling force of 10–20 pN sustained over a pulling distance range of 3–15 nm (Fig. 3), which will produce a work estimated to be  $15\text{ pN} \times 12\text{ nm} \sim 44k_B T$ —sufficient to overcome the energy barrier of  $>40 k_B T$  for membrane fusion ( $k_B$ : Boltzmann's constant;  $T$ : temperature).<sup>4</sup> By establishing a modeling framework for simulating the forced unfolding of SNARE, we will be able to address various mechanistic questions at amino-acid level of details, in particular how perturbations by point mutations may affect the zipping/unzipping activity of SNARE.

### ACKNOWLEDGMENTS

The simulations were conducted using the supercomputing cluster of Center for Computational Research at the University at Buffalo.

### REFERENCES

- Weber T, Zemelman BV, McNew JA, Westermann B, Gmachl M, Parlati F, Sollner TH, Rothman JE. SNAREpins: minimal machinery for membrane fusion. *Cell* 1998;92:759–772.
- Sutton RB, Fasshauer D, Jahn R, Brunger AT. Crystal structure of a SNARE complex involved in synaptic exocytosis at 2.4 Å resolution. *Nature* 1998;395:347–353.
- Sorensen JB, Wiederhold K, Muller EM, Milosevic I, Nagy G, de Groot BL, Grubmuller H, Fasshauer D. Sequential N- to C-terminal SNARE complex assembly drives priming and fusion of secretory vesicles. *EMBO J* 2006;25:955–966.
- Cohen FS, Melikyan GB. The energetics of membrane fusion from binding, through hemifusion, pore formation, and pore enlargement. *J Membr Biol* 2004;199:1–14.
- Brunger AT, Wenzinger K, Bowen M, Chu S. Single-molecule studies of the neuronal SNARE fusion machinery. *Annu Rev Biochem* 2009;78:903–928.
- Gao Y, Zorman S, Gundersen G, Xi Z, Ma L, Sirinakis G, Rothman JE, Zhang Y. Single reconstituted neuronal SNARE complexes zipper in three distinct stages. *Science* 2012;337:1340–1343.
- Sudhof TC, Rothman JE. Membrane fusion: grappling with SNARE and SM proteins. *Science* 2009;323:474–477.
- Fasshauer D, Eliason WK, Brunger AT, Jahn R. Identification of a minimal core of the synaptic SNARE complex sufficient for reversible assembly and disassembly. *Biochemistry* 1998;37:10354–10362.
- Fasshauer D, Otto H, Eliason WK, Jahn R, Brunger AT. Structural changes are associated with soluble N-ethylmaleimide-sensitive fusion protein attachment protein receptor complex formation. *J Biol Chem* 1997;272:28036–28041.
- Ellena JF, Liang B, Wiktor M, Stein A, Cafiso DS, Jahn R, Tamm LK. Dynamic structure of lipid-bound synaptobrevin suggests a nucleation-propagation mechanism for trans-SNARE complex formation. *Proc Natl Acad Sci U S A* 2009;106:20306–20311.
- Hayashi T, McMahon H, Yamasaki S, Binz T, Hata Y, Sudhof TC, Niemann H. Synaptic vesicle membrane fusion complex: action of clostridial neurotoxins on assembly. *EMBO J* 1994;13:5051–5061.
- Risselada HJ, Grubmuller H. How SNARE molecules mediate membrane fusion: recent insights from molecular simulations. *Curr Opin Struct Biol* 2012;22:187–196.
- Markvoort AJ, Marrink SJ. Lipid acrobatics in the membrane fusion arena. *Curr Top Membr* 2011;68:259–294.
- Knecht V, Grubmuller H. Mechanical coupling via the membrane fusion SNARE protein syntaxin 1A: a molecular dynamics study. *Biophys J* 2003;84:1527–1547.
- Durrieu MP, Lavery R, Baaden M. Interactions between neuronal fusion proteins explored by molecular dynamics. *Biophys J* 2008;94:3436–3446.
- Durrieu MP, Bond PJ, Sansom MS, Lavery R, Baaden M. Coarse-grain simulations of the R-SNARE fusion protein in its membrane environment detect long-lived conformational sub-states. *Chemphyschem* 2009;10:1548–1552.
- Wu S, Guo H. Simulation study of protein-mediated vesicle fusion. *J Phys Chem B* 2009;113:589–591.
- Risselada HJ, Kutzner C, Grubmuller H. Caught in the act: visualization of SNARE-mediated fusion events in molecular detail. *ChemBiochem* 2011;12:1049–1055.
- Lindau M, Hall BA, Chetwynd A, Beckstein O, Sansom MS. Coarse-grain simulations reveal movement of the synaptobrevin C-terminus in response to piconewton forces. *Biophys J* 2012;103:959–969.
- Karplus M, McCammon JA. Molecular dynamics simulations of biomolecules. *Nat Struct Biol* 2002;9:646–652.
- Tjong H, Zhou HX. The folding transition-state ensemble of a four-helix bundle protein: helix propensity as a determinant and macromolecular crowding as a probe. *Biophys J* 2010;98:2273–2280.
- Lu H, Israilewitz B, Krammer A, Vogel V, Schulten K. Unfolding of titin immunoglobulin domains by steered molecular dynamics simulation. *Biophys J* 1998;75:662–671.
- Liu Y, Hsin J, Kim H, Selvin PR, Schulten K. Extension of a three-helix bundle domain of myosin VI and key role of calmodulins. *Biophys J* 2011;100:2964–2973.
- Sabatini BL, Regehr WG. Timing of neurotransmission at fast synapses in the mammalian brain. *Nature* 1996;384:170–172.
- Feig M, Brooks CL, III. Recent advances in the development and application of implicit solvent models in biomolecule simulations. *Curr Opin Struct Biol* 2004;14:217–224.
- Schlitter J, Engels M, Kruger P. Targeted molecular dynamics: a new approach for searching pathways of conformational transitions. *J Mol Graph* 1994;12:84–89.
- Ovchinnikov V, Karplus M. Analysis and elimination of a bias in targeted molecular dynamics simulations of conformational transitions: application to calmodulin. *J Phys Chem B* 2012;116:8584–8603.
- Tozzini V. Coarse-grained models for proteins. *Curr Opin Struct Biol* 2005;15:144–150.
- Hinsen K. Analysis of domain motions by approximate normal mode calculations. *Proteins* 1998;33:417–429.

30. Atilgan AR, Durell SR, Jernigan RL, Demirel MC, Keskin O, Bahar I. Anisotropy of fluctuation dynamics of proteins with an elastic network model. *Biophys J* 2001;80:505–515.
31. Tama F, Sanejouand YH. Conformational change of proteins arising from normal mode calculations. *Protein Eng* 2001;14:1–6.
32. Tirion MM. Large amplitude elastic motions in proteins from a single-parameter, atomic analysis. *Phys Rev Lett* 1996;77:1905–1908.
33. Zheng WJ. Accurate flexible fitting of high-resolution protein structures into cryo-electron microscopy maps using coarse-grained pseudo-energy minimization. *Biophys J* 2011;100:478–488.
34. Zheng W, Tekpinar M. Accurate flexible fitting of high-resolution protein structures to small-angle X-ray scattering data using a coarse-grained model with implicit hydration shell. *Biophys J* 2011;101:2981–2991.
35. Zheng W, Tekpinar M. Analysis of protein conformational transitions using elastic network model. *Methods Mol Biol* 2014;1084:159–172.
36. Zheng W, Tekpinar M. Structure-based simulations of the translocation mechanism of the hepatitis C virus NS3 helicase along single-stranded nucleic acid. *Biophys J* 2012;103:1343–1353.
37. Tekpinar M, Zheng W. Coarse-grained and all-atom modeling of structural states and transitions in hemoglobin. *Proteins* 2013;81:240–252.
38. Tekpinar M, Zheng W. Predicting order of conformational changes during protein conformational transitions using an interpolated elastic network model. *Proteins* 2010;78:2469–2481.
39. Maragakis P, Karplus M. Large amplitude conformational change in proteins explored with a plastic network model: adenylate kinase. *J Mol Biol* 2005;352:807–822.
40. Zheng W, Brooks BR, Hummer G. Protein conformational transitions explored by mixed elastic network models. *Proteins* 2007;69:43–57.
41. Go N. Theoretical studies of protein folding. *Annu Rev Biophys Bioeng* 1983;12:183–210.
42. Brockwell DJ, Paci E, Zinober RC, Beddard GS, Olmsted PD, Smith DA, Perham RN, Radford SE. Pulling geometry defines the mechanical resistance of a beta-sheet protein. *Nat Struct Biol* 2003;10:731–737.
43. Lazaridis T, Karplus M. Effective energy function for proteins in solution. *Proteins* 1999;35:133–152.
44. Paci E, Karplus M. Unfolding proteins by external forces and temperature: the importance of topology and energetics. *Proc Natl Acad Sci U S A* 2000;97:6521–6526.
45. Brooks BR, Brooks CL, 3rd, Mackerell AD, Jr, Nilsson L, Petrella RJ, Roux B, Won Y, Archontis G, Bartels C, Boresch S, Caflisch A, Cavas L, Cui Q, Dinner AR, Feig M, Fischer S, Gao J, Hodoscek M, Im W, Kuczera K, Lazaridis T, Ma J, Ovchinnikov V, Paci E, Pastor RW, Post CB, Pu JZ, Schaefer M, Tidor B, Venable RM, Woodcock HL, Wu X, Yang W, York DM, Karplus M. CHARMM: the biomolecular simulation program. *J Comput Chem* 2009;30:1545–1614.
46. Karanicolas J, Brooks CL, III. Improved Go-like models demonstrate the robustness of protein folding mechanisms towards non-native interactions. *J Mol Biol* 2003;334:309–325.
47. Tekpinar M, Zheng WJ. Predicting order of conformational changes during protein conformational transitions using an interpolated elastic network model. *Proteins Struct Funct Bioinform* 2010;78:2469–2481.
48. Paci E, Karplus M. Forced unfolding of fibronectin type 3 modules: an analysis by biased molecular dynamics simulations. *J Mol Biol* 1999;288:441–459.
49. Fowler SB, Best RB, Toca Herrera JL, Rutherford TJ, Steward A, Paci E, Karplus M, Clarke J. Mechanical unfolding of a titin Ig domain: structure of unfolding intermediate revealed by combining AFM, molecular dynamics simulations, NMR and protein engineering. *J Mol Biol* 2002;322:841–849.
50. Hafner J, Zheng W. All-atom modeling of anisotropic atomic fluctuations in protein crystal structures. *J Chem Phys* 2011;135:144114.
51. Zheng W. Accurate flexible fitting of high-resolution protein structures into cryo-electron microscopy maps using coarse-grained pseudo-energy minimization. *Biophys J* 2011;100:478–488.
52. Song G, Jernigan RL. An enhanced elastic network model to represent the motions of domain-swapped proteins. *Proteins* 2006;63:197–209.
53. Hafner J, Zheng W. Optimal modeling of atomic fluctuations in protein crystal structures for weak crystal contact interactions. *J Chem Phys* 2010;132:014111.
54. Zimmermann MT, Leelananda SP, Gniewek P, Feng Y, Jernigan RL, Kloczkowski A. Free energies for coarse-grained proteins by integrating multibody statistical contact potentials with entropies from elastic network models. *J Struct Funct Genomics* 2011;12:137–147.
55. Gniewek P, Leelananda SP, Kolinski A, Jernigan RL, Kloczkowski A. Multibody coarse-grained potentials for native structure recognition and quality assessment of protein models. *Proteins* 2011;79:1923–1929.
56. Zhu X, Lopes PE, Mackerell AD, Jr. Recent developments and applications of the CHARMM force fields. *Wiley Interdiscip Rev Comput Mol Sci* 2012;2:167–185.
57. Walter AM, Wiederhold K, Bruns D, Fasshauer D, Sorensen JB. Synaptobrevin N-terminally bound to syntaxin-SNAP-25 defines the primed vesicle state in regulated exocytosis. *J Cell Biol* 2010;188:401–413.